Available online at www.sciencedirect.com
SCIENCE DIRECT®
Scripta Materialia 51 (2004) 509–514
Scripta MATERIALIA
www.actamat-journals.com

Relationship between grain size and Zener–Holloman parameter during friction stir processing in AZ31 Mg alloys

C.I. Chang, C.J. Lee, J.C. Huang *

Institute of Materials Science and Engineering, National Sun Yat-Sen University, Kaohisung, Taiwan 804, ROC

Received 24 March 2004; received in revised form 13 May 2004; accepted 25 May 2004
Available online 19 June 2004

Abstract

The relationship between the resulting grain size and the applied working strain rate and temperature for the friction stir processing in AZ31 Mg is systemically examined. The Zener–Holloman parameter is utilized in rationalizing the relationship. The grain orientation distribution is also studied using the X-ray diffraction.

Keywords: Friction stir processing; Magnesium alloy; Microstructure; Thermomechanical processing

1. Introduction

After the success and gradually wider applications of the friction stir welding (FSW) technique initially developed by The Welding Institute (TWI) in UK [1] in joining aerospace aluminum alloys, recent modifications into the friction stir processing (FSP) by Mishra et al. [2,3] also attract attention. FSP has been demonstrated to be an effective means of refining grain size of cast or wrought aluminum based alloys via dynamic recrystallization. A fine grain size in the typical range of 0.5–5 μm in the dynamically recrystallized zone of the FSP aluminum alloys has been widely reported [4–6]. Recently, extrafine grain sizes in the range of 30–180 nm have also been demonstrated [7].

Several grain size refinement processing means have been developed for light metals. The refined alloys are proven to be effective in enhancing room temperature mechanical properties, as well as low temperature or high strain rate superplasticity (LTSP or HSRSP). From the industrial point of view, hot rolling or extrusion processes are usually considered to be more economical and feasible.

The low formability nature of the Mg based alloys at room temperature with the hexagonal close-packed (HCP) crystal structure particularly requires grain refinement. It has been shown that the magnesium alloys with fine-grained structures become much more workable at slightly elevated temperatures such as 150–250 °C [7–11]. Such LTSP and/or HSRSP characteristics are expected to be applied in the 3C (computer, communication and consumer electronic) or automobile industry for the forming of complex components via pressing forming or press forging techniques.

The FSP technique may be powerful in refining the grain size and homogenize the microstructure (such as precipitates and dispersoids, or even the local solute compositions) in particular positions that need special attention. These can be the material locations needed to possess the highest forming limit or the greatest bending curvature. The FSP can also be only applied to selectively desired parts of a large work piece after previous secondary processing at room or elevated temperatures. It can also be used as a repair tool for sensitive parts.

The working temperature and strain rate, combined and expressed by the *Zener–Holloman* parameter,

* Corresponding author. Tel.: +886-7-525-2000x4063; fax: +886-7-525-4099.
E-mail address: jacobc@mail.nsysu.edu.tw (J.C. Huang).

1359-6462/$ - see front matter
doi:10.1016/j.scriptamat.2004.05.043

$Z = \dot{\varepsilon}\exp(Q/RT)$, where $\dot{\varepsilon}$ is the strain rate, R the gas constant, T the temperature, and Q the related activation energy, has been shown to impose influence on the resulting grain size in extruded Mg based alloys [11,12]. This parameter appears to be useful in predicting the resulting grain size and controlling the hot extrusion working parameters. In this paper, the assessment in using the *Zener–Holloman* parameter in FSP of the AZ31 Mg alloys is presented.

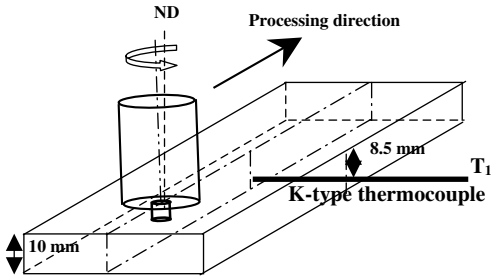

Fig. 1. Schematic drawing showing the inserted thermocouple positions in the FSP specimens.

2. Experimental methods

The AZ31B billets used in this study were purchased from the CDN Company, Deltabc, Canada. The chemical composition in mass percent is Mg–3.02%Al–1.01%Zn–0.30%Mn. This alloy is a solution hardened alloy with minimum precipitation. The as-received alloy was fabricated through semi-continuous casting and has the form of extruded billet measuring 178 mm in diameter and 300 mm in length. The billet possessed nearly equiaxed grains around 75 μm (all grain size hereafter was measured based on the linear line intercept method). One-step hot extrusion at 350 °C with an extrusion ratio of 20:1 was undertaken to produce a thick plate measuring 10 mm in thickness. The extruded plate contained a fully recrystallized equiaxed grain size of ~8 μm. Both the as-received billets and extruded plates are subjected to FSP.

The simplified FSP machine is a modified form of a vertical-type miller, with a 3 HP capability. The fixed pin tool is 6 mm in diameter and 6 mm in length. The shoulder diameter is 18 mm, and a 3° tilt angle of the fixed pin tool is applied (Fig. 1). The pitch distance is 1.5 mm. The advancing speed of the rotating pin was kept constant in this study to be 90 mm/min, with various rotation controls of the pin from 180 to 1800 rpm (rotation per minute). The plates were fixed by clamping kits and air cooling was applied. The working temperature was measured by the K-type thermocouple under the plates in T_1 place, as depicted in Fig. 1. During FSP, the temperature history is continuously recorded.

The Vickers hardness tests were conducted on the cross-sectional plane, using a Vickers indenter with a 200 gf load for 10 s. The grain structures of etched specimens were examined by optical microscopy (OM) or scanning electron microscopy (SEM). The texture was examined using X-ray diffraction (XRD) using Cu-Kα radiation. The X-ray beam was aligned to sample the cross-sectional plane of the billet, extruded plate, or FSP specimen.

3. Results and discussions

3.1. Grain sizes

Microstructure characterization in this study was focused on the dynamically recrystallized nugget zone. Fig. 2 shows the typical grain structures of the billet and extruded specimens after FSP. The grain shape observed from different cross-sectional planes is consistently of the equiaxed fully recrystallized type. The grain sizes near the bottom region of the dynamically recrystallized zone are typically smaller. For example, the grain sizes in the top, middle and bottom regions of the FSP extruded plate specimens at 180 and 1400 rpm are

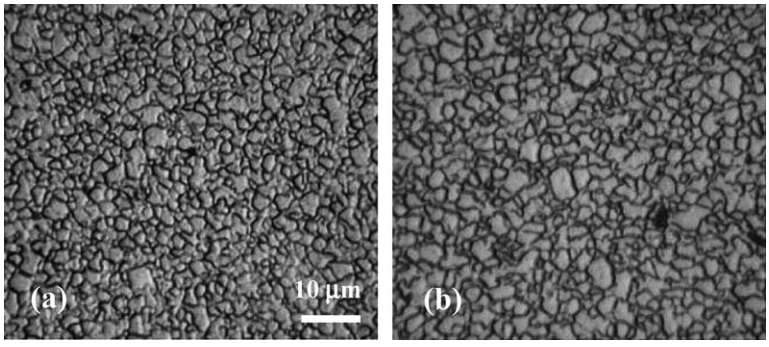

Fig. 2. OM micrographs of the fine grain structures in the recrystallized nugget zone: (a) billet specimens FSPed at 800 rpm, and (b) extrusion specimen FSPed at 800 rpm with a speed of 90 mm/min.

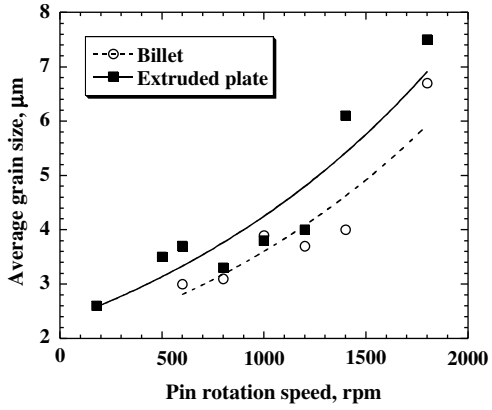

Fig. 3. Variation of the average grain size as a function of pin rotation speed for the FSP billet and extrusion specimens.

2.9/2.5/2.4 and 8.1/5.3/4.8 μm, respectively. The larger grain sizes in the top regime are due to the more severe temperature rise caused by the friction heat generated from the tool shoulder.

Due the lower initial hardness readings of the billet (H_v∼50) than those of the extruded plate (H_v∼65), the material flow resistance experienced in the billet specimens is slightly lower. This can be judged from the slightly lower temperatures experimentally measured from the FSP billet specimens, as described below. It follows that the resulting grain size in the billet specimens is sometimes even smaller than that of the extruded plate, though the initial grain size of the billet (∼75 μm) is considerably larger than the extruded plate (∼8 μm), as shown in Fig. 3.

3.2. Strain rates and temperatures

The material flow during FSP was driven by the rotating pin. The flow rate may be compatible to or lower than the rotation speed of the pin, since there would usually be a certain level of rotation lagging effect. By a simple linear assumption so that the average material flow rate, R_m, is about half of the pin rotational speed, R_p, the material flow strain rate, $\dot{\varepsilon}$, during FSP may be derived by the torsion typed deformation as

$$\dot{\varepsilon} = \frac{R_m \cdot 2\pi r_e}{L_e}, \quad (1)$$

where r_e and L_e are the effective (or average) radius and depth of the dynamically recrystallized zone. It is noted that all materials within the dynamically recrystallized zone would undergo the plastic flow, and such a zone appears to be an onion-like in shape. An effective radius, r_e, that can represent the average radius for all parts of the materials inside this zone, is assumed to equal about 0.78 (or π/4 [13]) of the observed zone boundary radius, r_b. Similar argument can also be applied to L. For a given R_p of 800 rpm (or 13.3 rps, rotation per second) with r_b∼3.5 mm and L_b∼6 mm, then $\dot{\varepsilon}$ can be calculated

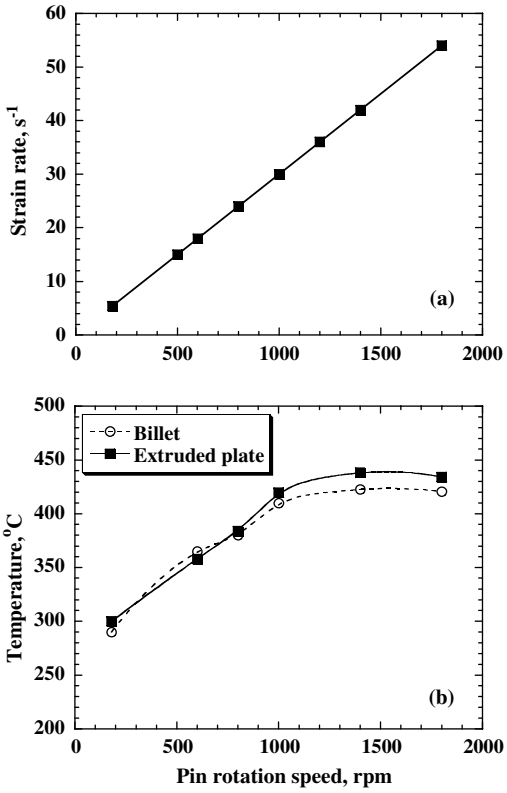

Fig. 4. Variation of the (a) strain rate and (b) temperature as a function of pin rotation speed.

to be ∼ 24 s^{-1}. The typical strain rates calculated for the current applied pin rotation speed from 180 to 1800 rpm are scattered within 5–50 s^{-1} (Fig. 4(a)), or in the neighborhood of 10^0–10^2 s^{-1}, depending on the actual zone size measured in each FSP specimen. This strain rate range is slightly higher than the processing strain rate previously adopted in our high-ratio extrusion experiments [10–12] (both ∼10^{-2}–10^1 s^{-1}).

The temperatures measured during FSP varied from 250 to 450 °C, depending on the FSP rotation speed (Fig. 4(b)). Typical recorded temperature profiles are shown in Fig. 5. The temperature rise duration is about 150 s. Such temperatures are compatible to those experienced during our previous hot extrusion research. And the resulting grain sizes can also be compared.

3.3. Relationship between grain size and Zener–Holloman parameter

In general, the average grain sizes would decrease with decreasing working temperature and increasing working strain rate. Within the present experiments, the finest grain size of ∼2.2 μm was obtained under a rotation speed of 180 rpm, or corresponding to a strain rate of 5.4 s^{-1} and a temperature of ∼300 °C.

The studies performed by Rhodes et al. [14] using the plunge and extract method of the rotating pin in the

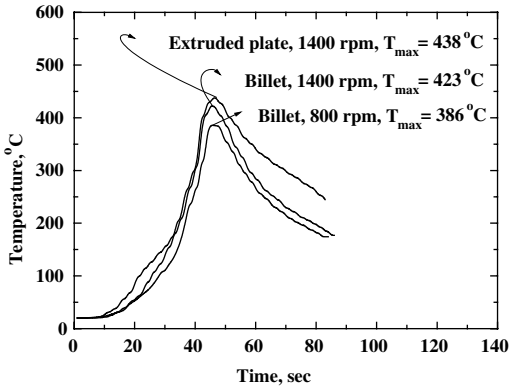

Fig. 5. Typical temperature profiles measured by the inserted thermocouple in the billet or extruded specimen FSPed at 800 or 1400 rpm with a speed of 90 mm/min.

7050 Al alloys have demonstrated that the fine grains in such FSP specimens are identical to those recrystallized grains in the annealed specimens at 350–450 °C for 1–4 min. This supports the argument that the fine grains in FSP specimens are a result of discontinuous dynamic recrystallization. Since the lattice and grain boundary diffusion rates of Mg at the working temperatures, for example, 300 °C, are 4.7×10^{-17} m^2/s and 2×10^{-20} δ m^3/s, respectively [15], (where δ is the grain boundary width), are much higher than the values of 1.8×10^{-17} m^2/s and 1.1×10^{-21} δ m^3/s for Al [15], the faster diffusion rate in the AZ series Mg alloys results in much faster and more complete dynamic recovery and dynamic recrystallization, and in turn results in fine-grained microstructures. The typical recrystallization temperatures are around 0.6–0.8 T_m (or around 300–450 °C) for Al alloys, and around 0.5–0.7 T_m (250–400 °C) for Mg counterparts. The latter temperatures are in fact the temperature ranges measured in this study.

In calculating the temperature compensated strain rate parameter, or the *Zener–Hollomon* Z parameter, during dynamic recrystallization, the activation energy Q for Mg lattice diffusion is about 135 kJ/mol [15]. The relationship between the *Zener–Hollomon* parameter and the average recrystallized grain size (d, in μm) for the AZ31 alloy during FSP is established, as shown in Fig. 6(a), and is given quantitatively by

$$\ln d = 9.0 - 0.27 \ln Z. \tag{2}$$

It should be noted that the ranges for d and Z in the current FSP study are still rather narrow, thereby the uncertainty is higher. Our previous analyses on the same AZ31 Mg alloys during warm extrusion or tensile loading [11,12] with wider ranges of d and Z have resulted in the same relationship but with slightly different constants, as

$$\ln d = 6.0 - 0.17 \ln Z, \tag{3}$$

as shown in Fig. 6(b). The current data on FSP still comfortably reside within the scattering band. In combining all the experimental data on the grain size and *Zener–Hollomon* parameter, it is found that the resulting grain sizes basically follow similar trends irrespective of the deformation path for extrusion, tension, or FSP.

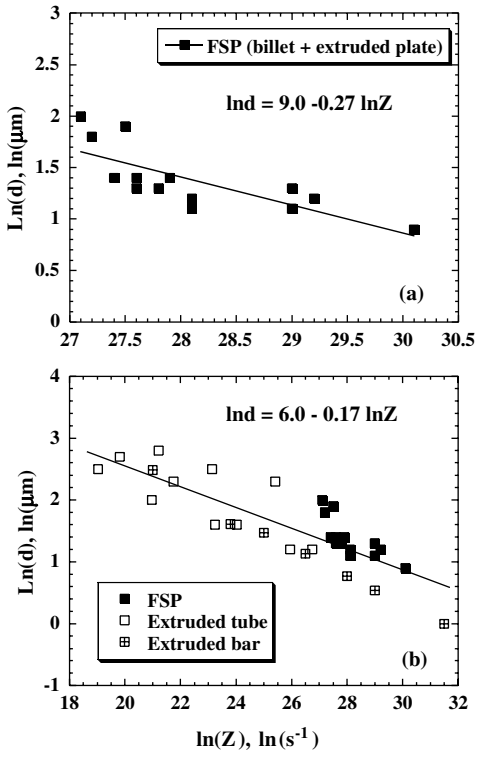

Fig. 6. Plots for the relationship between the resulting grain size and Zener–Holloman parameter in specimens processed by (a) FSP and (b) extrusion or tension. The data on FSP (solid square) are also included in (b) for comparison.

Sato et al. [16] also have attempted to relate the grain size in FSP 6063 Al alloys with the temperature experienced during FSP. The equation reached is [16]

$$\ln d = \ln\frac{At}{2} - \frac{Q}{2RT}, \tag{4}$$

where A is a constant and t is the time. Eq. (2) can also be expressed as

$$\ln d \approx 9 - \ln\frac{B\varepsilon}{t} - \frac{Q}{4RT} = K_1 + \ln K_2 t - \frac{Q}{4RT}, \tag{5}$$

where K_1 and K_2 are constants. The working time duration is coupled within the factor of working strain rate. The grain size dependence with temperature and strain rate (or time) during FSP can be easily compared with that experienced during other deformation histories.

3.4. Hardness measurements

The typical microhardness readings, H_v, in the various zones of the FSP specimens are depicted in Fig. 7. Based on systematic hardness measurements of the base

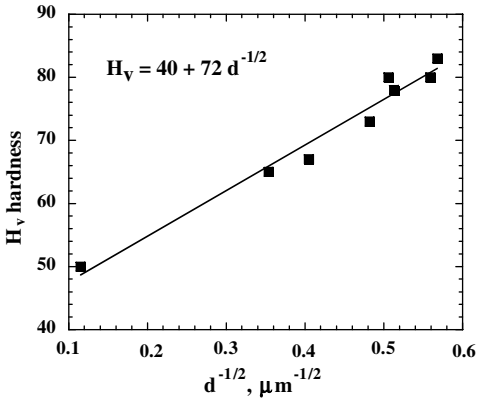

Fig. 7. Plot for the Hall–Petch relationship for the grain size induced by FSP.

and FSP specimens, the *Hall–Petch* relationship is well followed, i.e.,

$$H_v = 40 + 72d^{-1/2}. \quad (6)$$

3.5. Grain orientations

With strong dynamic recrystallization occurred during FSP in the current AZ31 Mg, the equiaxed fine grains exhibit much lower texture intensities as compared with the as-extruded AZ31 specimens [10–12]. Fig. 8 shows the computer simulated X-ray diffraction for a completely random Mg. The $(10\bar{1}0)$ and (0002) peak heights are about one half of the $(10\bar{1}1)$ peak height, all present within the 2θ angles of 30–40°.

The XRD diffraction patterns for the transverse cross-sectional plane of the as-received billet and its representative FSP specimens are shown in Fig. 9(a). The as-received billet exhibits basically nearly random grain orientation, reflecting its fully recrystallized coarse grained structure. As FSPed at a lower rotation speed of 800 rpm, the (0002) plane tends to lie on the transverse plane of the FSP specimen (perpendicular to the pin travel direction and parallel to the onion back surface, as also observed by Park et al. [17]). With increasing rotation speed to 1400 or 1800 rpm, the $(10\bar{1}1)$ peak height increases slightly, but never approaching to the random case.

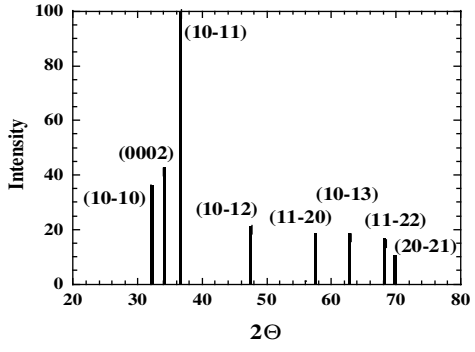

Fig. 8. Simulated X-ray diffraction pattern for the completely random Mg using the Cu-Kα radiation. The vertical axis is for the X-ray intensity. Within the 2θ angles of 30–40°, the $(10\bar{1}0)$ and (0002) peak heights are about one half of the $(10\bar{1}1)$ peak height.

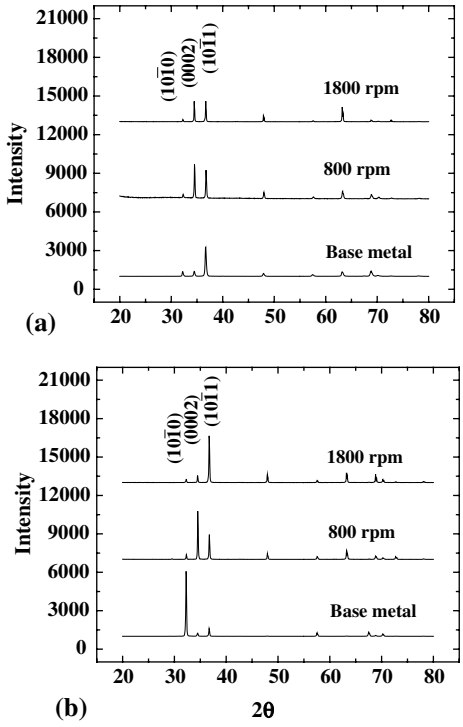

Fig. 9. X-ray diffraction patterns obtained from (a) billet and (b) extruded plate specimens before or after FSP with a rotation speed of 800 or 1800 rpm.

The representative XRD results for the extruded specimens are presented in Fig. 9(b). The $(10\bar{1}0)$ peak is significantly strong in the extruded plate (before FSP), suggesting that $(10\bar{1}0)$ plane is parallel to the transverse plane or the (0002) plane is lying on the extrusion flat plane of the extruded plate. To align the (0002) basal plane on the rolling or extrusion flat plane is typical for the hexagonal Mg alloys [18]. Upon FSPed at 800 rpm, a complete different texture with the (0002) plane now lying on the transverse plane is seen, similar to the case above for the billet specimens FSPed at 800 rpm. As FSPed at a much higher rotation speed of 1400 or 1800 rpm, the induced higher temperature rise (Fig. 4(b)) results in more complete dynamic recrystallization, as well as more random orientation, almost approaching to the pattern shown in Fig. 8.

4. Conclusion

The relationship between the resulting grain size and the applied working strain rate and temperature for the friction stir processing in the AZ31 Mg alloy is systemically examined. The Zener–Holloman parameter is

utilized in rationalizing the relationship, and it was found that the relationship of $\ln d = 9.0 - 0.27 \ln Z$ is followed. The temperature rise during FSP is traced, and the maximum temperature can reach 250–450 °C, depending on the FSP pin rotation speed. X-ray diffraction results show that, in the FSP dynamically recrystallized zone, the (0002) basal plane tends to lie on the transverse plane at lower pin rotation speeds, and approaches to nearly random orientation at higher rotation speeds.

Acknowledgment

The authors are gratefully acknowledge the sponsorship by National Science Council of Taiwan, ROC, under the project no. NSC 92-2216-E-110-020.

References

[1] Thomas WM, Nicholas ED, Needham JC, Church MG, Templesmith P, Dawes CJ. Intl Patent No. PCT/GB92/02203.
[2] Mishra RS, Mahoney MW, McFadden SX, Mara NA, Mukherjee AK. Scripta Mater 2000;42:263.
[3] Ma ZY, Mishra RS, Mahoney MW. Acta Mater 2002;50:4419.
[4] Kwon YJ, Shigematsu I, Saito N. Scripta Mater 2003;49:785.
[5] Rhodes CG, Mahoney MW, Bingel WH, Spurling RA, Bampton CC. Scripta Mater 1997;36:69.
[6] Charit I, Mishra RS. Mater Sci Eng A 2003;359:250.
[7] Su JQ, Nwlson TW, Sterling CJ. J Mater Res 2003;18:1757.
[8] Matsubara K, Miyahara Y, Horita Z, Langdon TG. Acta Mater 2003;51:3073.
[9] Watanabe H, Mukai T, Ishikawa K, Higashi L. Scripta Mater 2002;46:851.
[10] Lin HK, Huang JC. Mater Trans 2002;43:2424.
[11] Wang YN, Lee CJ, Lin HK, Huang TT, Huang JC. Mater Sci Forum 2003;426–432:2655.
[12] Huang CC, Huang JC, Lin IK, Hwang YM. Key Eng Mater. in press.
[13] Ardell AJ. Metall Trans A 1985;16A:2131.
[14] Rhodes CG, Mahoney MW, Bingel WH, Calabrese M. Scripta Mater 2003;48:1451.
[15] Forst HJ, Ashby MF. In: Deformation-Mechanism Maps. Oxford: Pergamon Press; 1982. p. 21 and p. 44.
[16] Sato YS, Urata M, Kokawa H. Metall Mater Trans A 2002;33:625.
[17] Park SHC, Sato YS, Kokawa H. Metall Mater Trans A 2003;34:987.
[18] Wang YN, Huang JC. Mater Chem Phys 2003;81:11.